ELSEVIER

Biochimica et Biophysica Acta 1191 (1994) 354–361

BBA Biochimica et Biophysica Acta

Effect of vesicle composition and curvature on the dissociation of phosphatidic acid in small unilamellar vesicles – a ^{31}P-NMR study

Manal A. Swairjo [a], Barbara A. Seaton [a,*], Mary F. Roberts [b]

[a] *Department of Physiology, Boston University School of Medicine, 80 East Concord St., Boston, MA 02118, USA*
[b] *Department of Chemistry, Boston College, Chestnut Hill, MA 02167, USA*

(Received 29 June 1993; revised manuscript received 2 November 1993)

Abstract

Sonicated small unilamellar vesicles (SUVs) containing phosphatidic acid (PA) give two PA ^{31}P-NMR resonances corresponding to PA molecules in the inner and outer leaflets of the bilayer. This NMR differentiation between the two monolayers is not due to a pH gradient across the membrane but instead reflects differential packing in the inner and outer leaflets imposed by the highly curved SUV surface. The apparent pK_a of the outer-leaflet PA increases with decreasing surface curvature and with increasing PA content. The estimated relationship between the apparent pK_a of the outer-leaflet PA headgroup and vesicle curvature may provide a qualitative probe for effects related to surface curvature in these model-membrane systems.

Key words: Liposome; Phosphatidic acid; NMR, ^{31}P-; Electron microscopy; Vesicle

1. Introduction

Bilayer-forming lipids have been used extensively to prepare model systems that can be readily manipulated to elucidate some of the physical and chemical properties of biological membranes. Model-membrane systems such as multilamellar vesicles [1], large [2,3] and small [4,5] unilamellar vesicles have been used to study lipid–protein interactions in membranes [6], membrane fusion [7], interfacial catalysis [8] and drug delivery and targeting [9]. A particularly useful technique to characterize unilamellar vesicles of various lipids and the mechanisms of their formation has been nuclear magnetic resonance (NMR) spectroscopy [10–12].

Recently, a family of cytosolic proteins that bind to membranes containing negatively charged phospholipids in a calcium-dependent manner was discovered in eukaryotic cells. In order to study the effects exerted by these proteins, termed annexins, on membrane bilayer headgroups using NMR spectroscopy, an appropriate model membrane system had to be developed. An additional constraint for these studies is that free calcium often causes aggregation and fusion of vesicles containing anionic phospholipids [3,13]. The model membrane system therefore had to contain negatively charged phospholipids, tolerate millimolar calcium levels, and give rise to distinct and interpretable NMR features. The model chosen, PA/PC SUVs, met these criteria. PA is unique among the various acidic phospholipids since it (i) has a pK_a in the physiological pH range, (ii) forms stable small unilamellar vesicles (SUVs) when mixed with phosphatidylcholine (PC) and sonicated in aqueous solutions and (iii) exhibits a ^{31}P-NMR resonance easily resolved from that of PC at high magnetic field. Hence both pH sensitivity and resolution may be exploited in ^{31}P-NMR studies of the interaction of peripheral membrane proteins such as annexins with lipid bilayers. The present paper provides NMR characterization of this useful model membrane system.

* Corresponding author. Fax: +1 (617) 6384273.

Abbreviations: PA, 1,2-dioleoyl-*sn*-glycero-3-phosphate; PC, 1,2-dioleoyl-*sn*-glycero-3-phosphocholine; SUV, small unilamellar vesicle; LUV, large unilamellar vesicle; FCCP, carbonyl cyanide *p*-(trifluoromethoxy)phenylhydrazone; NMR, nuclear magnetic resonance; DTT, dithiothreitol; EM, electron microscopy; Hepes, 4-(2-hydroxyethyl)-1-piperazineethanesulfonic acid.

SSDI 0005-2736(94)00009-E

2. Materials and methods

Synthetic 1,2-dioleoyl-*sn*-glycero-3-phosphocholine (PC) and 1,2-dioleoyl-*sn*-glycero-3-phosphate monosodium salt (PA) were purchased from Avanti Polar Lipids (Birmingham, AL, USA) and used without further purification. The proton ionophore carbonyl cyanide *p*-(trifluoromethoxy)phenylhydrazone (FCCP) was purchased from Sigma (St. Louis, MO, USA). Small unilamellar vesicles (SUVs) were prepared as follows. PA, PC, and mixtures of PA/PC in various molar ratios (5:1, 3:1, 1:1, 1:3, and 1:5) were dried from chloroform solutions under nitrogen and then lyophilized. The amount of PA in all these mixtures was kept constant. The phospholipid mixtures were then suspended in buffer (50 mM Hepes, 100 mM KCl, 0.1 mM DTT, and 0.02% NaN_3, pH 7.4) such that the final concentration of PA was 16 mM. The lipid suspensions were sonicated under standard conditions for an interval of 7–9 min using a Branson W-350 sonicator with a microtip. Large lipid structures were separated by centrifugation at $17000 \times g$ for 60 min and discarded. Samples were kept under nitrogen/argon during all steps of preparation. The purity of the phospholipids after sonication was checked by ^{31}P-NMR on $CDCl_3$ solutions of $CHCl_3/CH_3OH$-extracted PA. The final phospholipid concentrations were checked by the ashing procedure for total phosphate according to the method of Ames and Dubin [14].

Large unilamellar vesicles (LUVs) containing PA/PC in 1:1 molar ratio were prepared according to the method of MacDonald et al. [15]. Lipid suspensions in buffer (pH 7.4 or pH 8.95) were extruded through a polycarbonate membrane using a manual LiposoFast extruder (Avestin, Ottawa, Canada). LUVs with diameters in the range 450–550 Å were extruded through a membrane with a pore size of 50-nm. To avoid formation of multilamellar structures, low concentration (3 mM) lipid suspensions were extruded and the resulting LUVs suspensions were transferred into Centricon-100 centrifugal microconcentrator tubes (Amicon, MA, USA) with membranes of molecular-weight cut-off of 100000. The microconcentrators were prewashed with 0.1 M NaOH followed by three washes with buffer. The LUVs suspensions were concentrated by ultrafiltration at $755 \times g$ to a final concentration of 32 mM. The resulting retentates were assayed for total phosphate as mentioned above.

The morphology and size distribution of the vesicles were checked by negative-stain electron microscopy (EM). 8 μl of a diluted sample of sonicated or extruded vesicles containing 0.1 mM PA/PC 1:1 was pipetted onto a glow-discharged carbon-coated 300-mesh copper grid and followed by 8 μl of 1% phosphotungstic acid (pH 7.4). After air-drying the grid was viewed and imaged using a calibrated Philips CM-12 transmission electron microscope. A sample of SUVs containing 30 mM of PA/PC (1:1) and 1 mM $CaCl_2$ was diluted in buffer to 0.1 mM total phospholipid and a grid was prepared as above.

Light scattering was measured to test for possible vesicle aggregation in the presence of calcium. A fresh sample (0.5 ml) of SUVs containing 23 mM total lipid was placed in a 2 mm-thick glass cuvette and its optical density at 600 nm was measured using a Perkin-Elmer Lambda 2 UV/VIS spectrometer. The optical density of the sample was monitored every 30 s for 10 min. 1 mM $CaCl_2$ was added and the optical density at 600 nm was monitored every 30 s for the initial 50 min and every 5 min for 5 more hours. As a control, 5 mM $CaCl_2$ was added to a similar preparation and the sample was monitored every 15 s for 50 min, then every 15 min for the following 5 h. A calcium-free control was also monitored in a similar fashion for 5 h.

WALTZ ^{1}H-decoupled ^{31}P (202.33 MHz) spectra were recorded on a Varian Unity 500 spectrometer using a 6 kHz sweep width, 9344 data points, 90° flip angle, 0.779 s acquisition time, 20 Hz line broadening, and 200 transients. For locking purposes vesicle stock suspensions were slightly diluted with ^2H_2O (99.98% atom D) to final concentrations of 28–30 mM. A ^{31}P-NMR spectrum was taken for each of the above SUVs preparations at pH 7.4. The sample was then titrated with DCl/NaOD (Sigma, St. Louis, MO, USA) to a pH in the range 5.0–13.0 and a ^{31}P-NMR spectrum was taken after each titration. ^{31}P measurements of PA/PC (1:1) LUVs were performed on a Varian Unity 300 operating at a ^{31}P frequency of 121.4 MHz and using a 16.5 kHz sweep width, 59904 data points, 8.0 μs pulse width, 1.815 s acquisition time, 5 Hz line broadening, and 20000 transients. Phosphoric acid was used as an external reference in all experiments. All measurements were performed at room temperature. Spectral deconvolutions were done using the 'fitspec' protocol of the Varian VNMR software and spectra were fit with Lorentzian lineshapes.

3. Results

Visible-light scattering by SUVs is qualitatively represented by the optical density at 600 nm. In Fig. 1 is shown the optical density at 600 nm for a SUV preparation containing 23 mM PA/PC in 1:1 molar ratio as monitored during an interval of 3 h after adding 1 mM $CaCl_2$. The constant optical density indicates vesicle stability and negligible aggregation into larger particles. In the control experiment, 5 mM $CaCl_2$ was added to an identical SUV sample and monitored for the same period of time. A rapid increase in the optical density occurred within the first 1.5–2 min. This can be correlated with the formation of particles with diame-

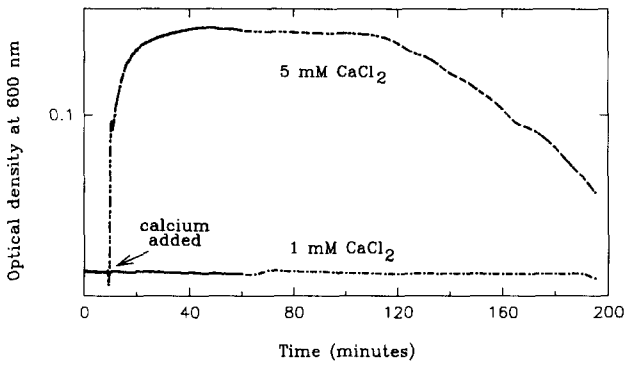

Fig. 1. Effect of 1 mM $CaCl_2$ on the optical density at 600 nm of a suspension of sonicated SUVs containing a 23 mM mixture of PA and PC in 1:1 molar ratio (pH 7.4). In the control experiment 5 mM $CaCl_2$ was added.

ters less than one-tenth of the wavelength, consistent with a Rayleigh scattering phenomenon (valid for solid, homogeneous spheres). These particles may be fusing dimers and trimers of the 200-Å SUVs (actual size range is 150–250 Å in diameter). The optical density of the suspension then slowly decreases with time which is typical for particles of increasing size. Such a decrease is characteristic of Mie scattering [16]. The decrease in optical density continues at a higher rate after 2 h of adding calcium, as large particles start sedimenting out of the optical path. This loss of optical density can be reversed by stirring the sample. Similar optical density changes were observed for pure PA SUVs at calcium concentrations higher than 300 μM.

A more quantitative analysis of vesicle sizes is provided by EM. The electron micrographs of a preparation of SUVs containing PA/PC in 1:1 molar ratio revealed a relatively homogeneous population of perfectly round vesicles with diameters in the range 150–250 Å (Fig. 2a). 1 mM $CaCl_2$ did not significantly affect the shapes of SUVs (Fig. 2b). Comparison of size-distribution histograms obtained from a number of such electron micrographs for SUVs without calcium (Fig.

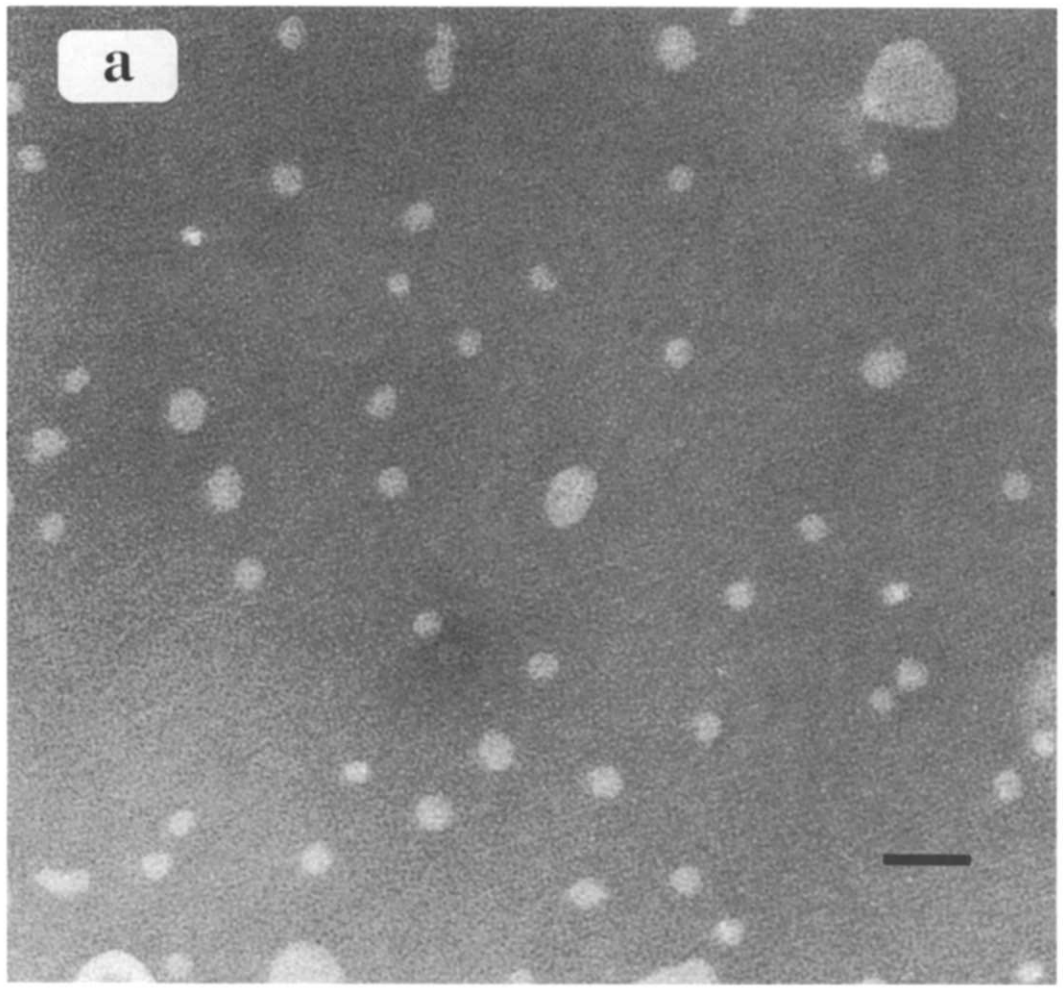

Fig. 2. Negative-stain electron micrographs of sonicated SUVs containing PA/PC (1:1), pH 7.4 under different conditions. (a) No calcium added. (b) In the presence of 1 mM $CaCl_2$. The original 30 mM sonicated phospholipid sample was diluted 1:300 in buffer. The bar indicates 50 nm. The magnification factor is 240 000.

3a) and SUVs with 1 mM $CaCl_2$ (Fig. 3b) shows a slight increase in the larger-vesicle population (230–300 Å) in the presence of 1 mM $CaCl_2$. However, close to 70% of the vesicles in both preparations are in the same size range, 150–220 Å. This confirms the negligible effect of 1 mM $CaCl_2$ on the integrity of the vesicles (30 mM total phospholipid) in that size range. Panel (c) in Fig. 3 shows the diameter distribution of the LUVs prepared by extrusion in pH 7.4 buffer through a 50-nm pore-size polycarbonate membrane.

The high-resolution ^{31}P-NMR spectrum of a sample of sonicated SUVs containing 30 mM of a PA/PC (1:1) mixture at pH 7.4 consists of a single PC resonance at −0.64 ppm (relative to 80% phosphoric acid) and a downfield doublet corresponding to the PA phosphate at 0.38 and 1.28 ppm (Fig. 4). After spectral deconvolution assuming Lorentzian lineshapes, the intensity ratio of the PA resonance at 1.28 ppm to that at 0.38 ppm was found to be 2:1. The linewidths of the PC and the downfield PA resonances are 162 and 170 Hz (error = ±20 Hz), respectively. A similar SUV sample with 1 mM $CaCl_2$ added gives a ^{31}P spectrum with identical features and linewidths. Upon gradually titrating the sample with NaOD, the downfield PA resonance shifted further downfield to 2.82 ppm at pH 8.1 and 4.05 ppm at pH 12.3. The upfield PA resonance remained relatively unaffected by the solution pH. The inaccessibility of the upfield resonance to pH suggested it belonged to the phosphorus of the inner-leaflet PA molecules in the bilayer. The downfield component of the doublet would then correspond to the outer-leaflet PA molecules. The integrity of the vesicles during the course of the experiment was confirmed by the similar vesicle size distributions obtained for the pH 7.4 and pH 9.0 samples when sized with EM (data not shown).

A possible cause for the NMR separation of the inner- and outer-leaflet PA molecules is an actual pH gradient across the bilayer. Such a pH gradient could have arisen from limited lipid hydrolysis during sonication. To investigate this possibility, the proton ionophore FCCP was introduced into the lipid bilayer by drying a mixture of 50 μM FCCP and 32 mM phospholipid and suspending and sonicating the mix-

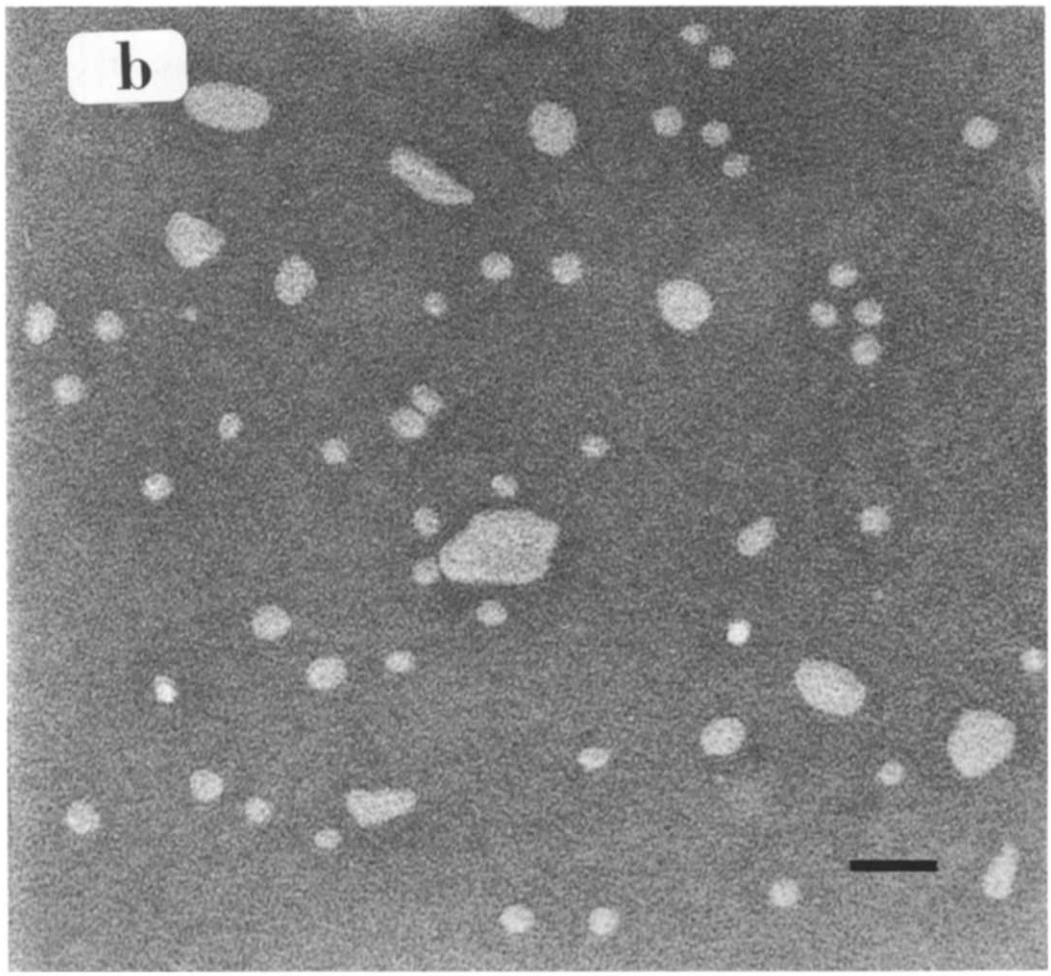

Fig. 2 (continued).

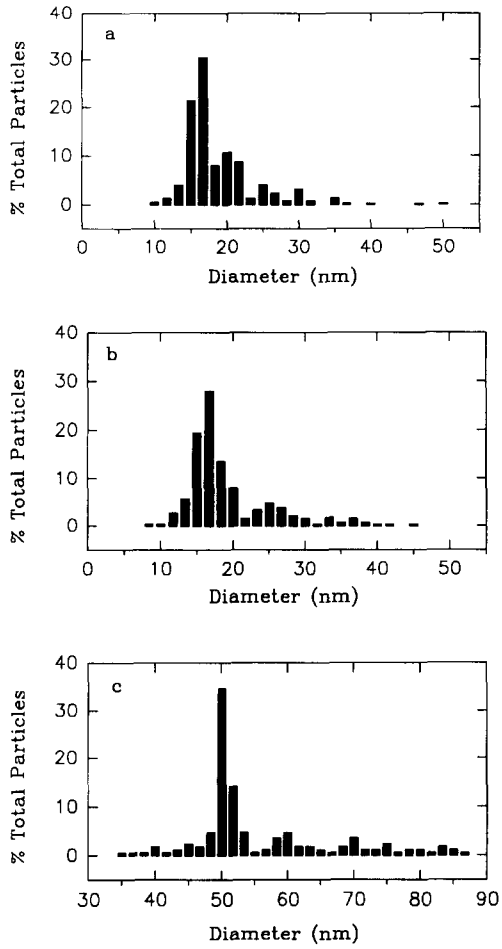

Fig. 3. Diameter distribution of sonicated SUVs containing PA/PC (1:1), pH 7.4 in the absence (a) and presence (b) of 1 mM $CaCl_2$. Panel (c) shows the diameter distribution of vesicles extruded through a 50-nm pore-size polycarbonate membrane (pH 7.4). Particles from multiple electron micrographs as those in Fig. 2 were sized. In each panel a total of 340 particles were counted.

ture in buffer. Given the observed vesicle-size distribution, a typical vesicle contained an average of 10 FCCP molecules. These vesicles produced ^{31}P-NMR spectra with the same features as those discussed above, i.e., an upfield PA resonance that is still insensitive to pH in the range 6.5–13.5 (Fig. 5). In addition, an FCCP-free sample of PA/PC (1:1) SUVs was resonicated for 1 min after each titration with NaOD. During resonication the vesicles break and reform and the media inside and outside the SUV mix, resulting in equal pH on both sides of the membrane. This treatment yielded both a similar titration curve for the outer-leaflet PA and insensitivity of the inner-leaflet PA to pH changes (Fig. 5). These results, consistent with those obtained with FCCP-containing SUVs, confirm that there is no apparent pH gradient across the membrane in these vesicle preparations.

The insensitivity of the inner-PA band to pH titrations in the range 6.5–13.5 despite its accessibility to H^+ (or OH^-) can be attributed to the high pK_a of that PA headgroup. The latter is due to a specific chemical environment set by the tight geometry of the highly curved inner surface of the SUV. In an attempt to investigate the effect of vesicle curvature on the NMR differentiation of the inner- and outer-leaflet PA, lower-field ^{31}P spectra were obtained from a sample of sonicated SUVs (250 Å, pH 8.95) and another of extruded LUVs (500 Å, pH 8.95) (Fig. 6). The linewidth of the PC resonance from LUVs and SUVs is 154 and 34 Hz (error = ±5 Hz), respectively. SUVs and LUVs prepared at these conditions gave size distributions similar to those in Fig. 3(a) and (c). In the ^{31}P-NMR spectrum of LUVs, a single large PA resonance at 2.9 ppm replaces the downfield doublet at 3.24 ppm and 1.97 ppm observed in the ^{31}P spectrum of SUVs. The intensity of this single resonance is equal to the sum of intensities of the doublet components. Deconvolution of the LUV spectrum gives rise to only one PA peak at 2.9 ppm with a linewidth of 310 Hz. This fact, together with the observation that the chemical shift of the PA

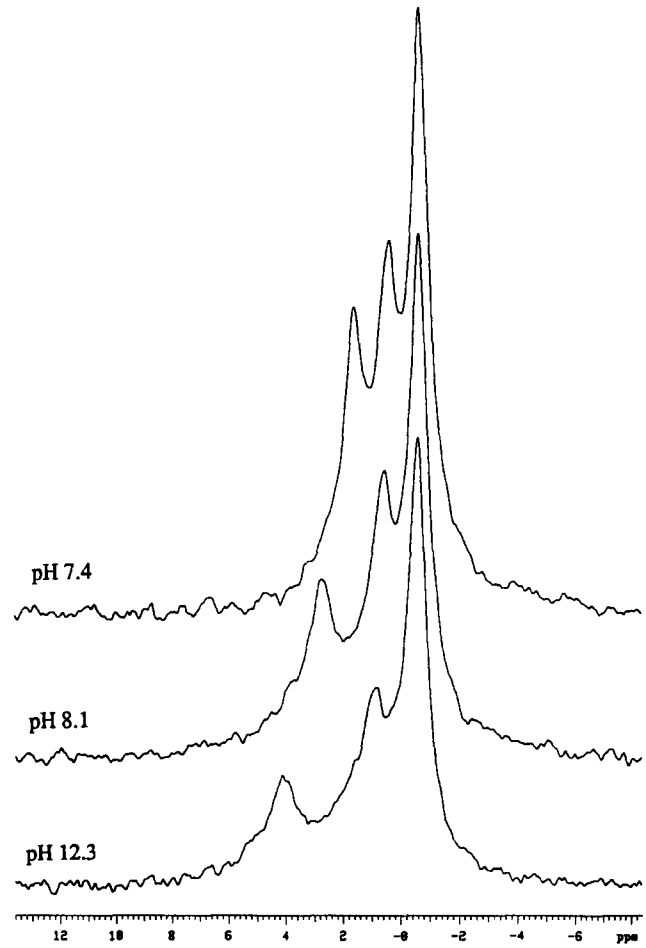

Fig. 4. ^{31}P-NMR (202 MHz) spectra of SUVs containing a mixture of PA/PC in 1:1 molar ratio prepared by sonicating the aqueous lipid suspension at pH 7.4. The lower two spectra correspond to the same SUV sample adjusted with NaOD to pH 8.1 and 12.3.

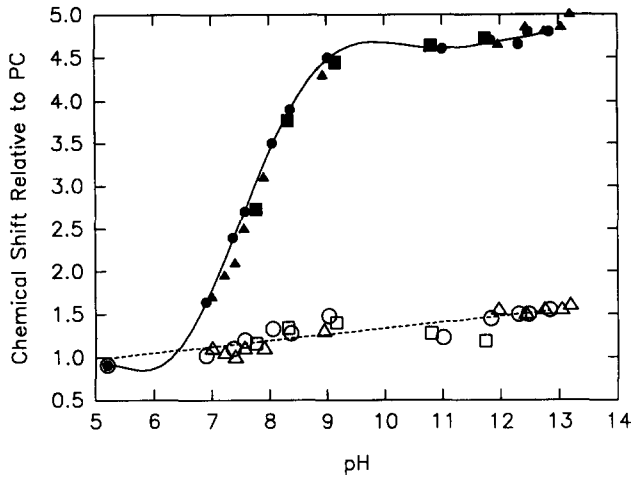

Fig. 5. Titration curves of different lipid dispersions. The ^{31}P chemical shift of the outer-leaflet PA molecules (filled symbols) and the inner-leaflet PA (hollow symbols) measured relative to the invariant PC chemical shift is shown as a function of the apparent pH. ●, ○: sonicated SUVs containing 32 mM PA/PC (1:1). ▲, △: sonicated SUVs containing 32 mM PA/PC (1:1) and 50 μM FCCP. ■, □: sonicated SUVs containing 32 mM PA/PC (1:1) and resonicated after each titration with NaOD.

molecules in the LUV lies at an intermediate position between the chemical shifts of the inner- and outer-leaflet PA molecules of the SUV, suggests that the same two PA populations are not NMR-resolvable in the LUV relative to the case of the SUV at the same pH.

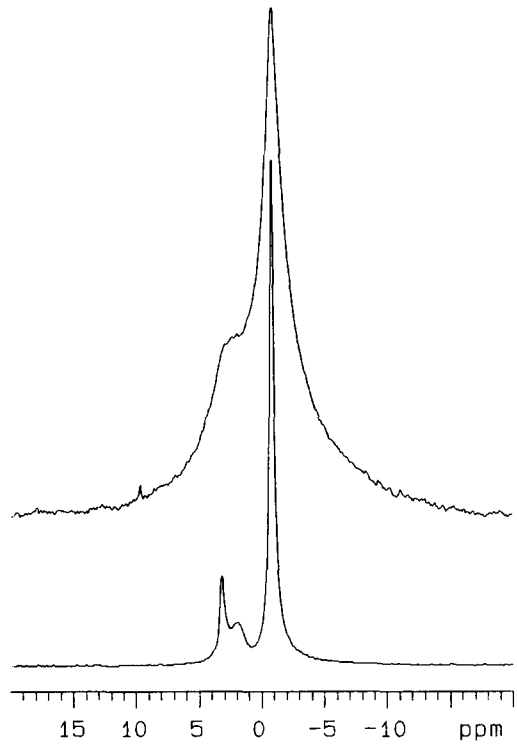

Fig. 6. ^{31}P-NMR (121.4 MHz) spectra of 28 mM PA/PC (1:1) 500-Å LUVs (top) and 250-Å SUVs (bottom). The SUVs were prepared by sonication in pH 8.95 buffer. The LUVs were prepared by extrusion through a 50-nm pore-size polycarbonate membrane in the same buffer.

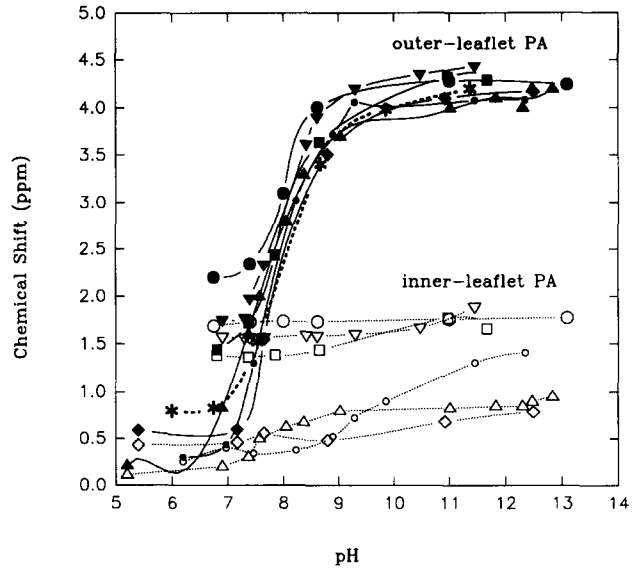

Fig. 7. Titration curves of sonicated dispersions of PA/PC mixtures with different amounts of PC and a fixed final PA concentration of 16 mM. The ^{31}P chemical shift of the outer-leaflet PA (filled symbols) and the inner-leaflet PA (hollow symbols) measured relative to 80% phosphoric acid is shown as a function of the apparent pH. ●/○: SUVs containing pure PA. The rest correspond to SUVs containing PA/PC mixtures in the following ratios: 5:1 (▼, ▽), 3:1 (■, □), 1:1 (▲, △), 1:3 (◆, ◇), 1:5 (●, ○). The symbol * is used to designate the outer-leaflet PA of PA/PC (1:1) LUVs prepared by extrusion through a 50-nm polycarbonate membrane (pH 7.4), 16 mM final PA concentration.

pH titration experiments were conducted on sonicated SUVs containing increasing amounts of PC and on LUVs extruded through a 50-nm pore-size polycarbonate membrane. The PA concentration is 16 mM in all preparations. The changes in the chemical shifts of both the outer-leaflet and inner-leaflet PA headgroups with pH were used to generate a pH titration curve for each SUV preparation. Fig. 7 shows the pH titration curves in the range 5.0–13.5 of sonicated SUVs containing pure PA or mixtures of PA/PC with PC content increasing from 0–83%. Based on measurements of 4 different samples for each PC content, the root-mean-square error in the chemical shift is ±0.1 ppm and ±0.3 ppm in the pH ranges 6.0–13.0 and 5.0–6.0, respectively. These curves give an apparent pK_a value of the outer-leaflet PA headgroup which decreases linearly with increasing PC content of the SUV (Fig. 8). The average uncertainty in the apparent pK_a estimates is ±0.1 pH units. The linearity of the pK_a-versus-PC-percentage plot indicates that the phospholipids are mixing in the bilayer. Instability of vesicles containing more than 50% PA at acidic pH made it difficult to obtain low-pH data for such vesicles. The inner- and

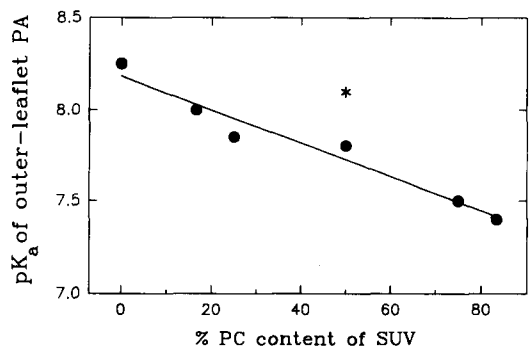

Fig. 8. The dependence of the apparent pK_a value of the outer-leaflet PA, derived from the titration curves of Fig. 7, on the PC content in the SUV (●). The point (*) corresponds to the pK_a of the outer-leaflet PA in 500-Å LUVs containing 50% PC, derived from the corresponding titration curve in Fig. 7.

outer-PA chemical shifts overlap at acidic pH, indicating that the inner-leaflet PA is almost entirely in a monoanionic form. In the acidic pH range, the outer-leaflet PA chemical shift generally decreases with increasing PC content at a given pH. Also, the chemical shift of the inner-leaflet PA decreases with increasing PC content in the SUV. There are two possible explanations for this observation. (i) If the ^{31}P chemical shifts primarily reflect the net ionization state of PA, the above observations indicate that as the PC content increases in the SUV, the equilibrium between the monoanionic and dianionic PA forms is shifted toward the dianionic form at a given pH. The headgroup area for dianionic PA is larger than that for monoanionic PA. If packing is critical to the stability of the SUV then with increasing separation between the PA molecules in the outer leaflet the need for the larger-headgroup PA form increases, thus a small amount of the dianionic PA form is favored even at acidic pH. (ii) Alternatively, factors other than the ionization state of PA can contribute to its ^{31}P chemical shift. Local surface charge may be one such factor. Monoanionic PA in SUVs with more than 50% PC may sense either the positively charged *N*-methyl moiety or the lower net negative surface charge, and this could lead to an upfield (i.e., shielded) value for the monoanionic-PA chemical shift. Regardless of which explanation is correct, the net result is a decrease in apparent pK_a as the PC content of the SUV increases.

In PA/PC (1:1) LUVs, the outer-leaflet PA ^{31}P resonance also shifts downfield with increasing pH (Fig. 7), giving rise to an apparent pK_a of 8.1 ± 0.1. This apparent pK_a value is higher than that estimated for the outer-leaflet PA in PA/PC (1:1) SUVs (7.8) which may indicate a closer packing of the PA headgroups in the LUV outer leaflet than in the SUV outer leaflet even though the two vesicle systems have the same phospholipid composition.

4. Discussion

Small unilamellar vesicles of PA produced by sonication give rise to two ^{31}P resonances. The downfield signal corresponds to phosphatidic acid molecules on the outer leaflet of the bilayer and the upfield signal corresponds to the inner leaflet. Two PA resonances appeared in spectra of sonicated phospholipid dispersions with up to 83% PC. Assignments of the PA resonances to the inner and outer leaflets are based on the relative intensities of the two PA components and on the titratability of the downfield signal with pH. These assignments are consistent with those reported by other groups [17,18]. In LUVs only a single PA resonance is observed. Although the linewidths are considerably larger in the LUV spectrum than the SUV spectrum, deconvoluted ^{31}P spectra of LUVs prepared from aqueous phospholipid dispersions at pH 7.4 (data not shown) and pH 8.95 give one PA resonance. This resonance is upfield to the outer-leaflet PA component in the SUV spectrum at the same pH. This is consistent with the increase in the apparent pK_a of the outer-leaflet PA in the LUV relative to its value in the SUV. As the surface curvature decreases with increasing vesicle size, the outer-leaflet PA headgroups are brought closer together which translates into an increase in apparent pK_a. Also, the inner-leaflet molecules are subjected to a geometry which resembles that on the outside. This may explain the presence of a single PA resonance rather than a doublet in the LUV spectrum.

The chemical shift of PA can be directly related to the apparent pH using the pH titration curves of Fig. 7. Since there is no apparent pH gradient across the membranes of vesicles prepared in pH 7.4 buffer, we attribute the difference in the ^{31}P chemical shifts of the PA molecules in the two monolayers (Fig. 4, top spectrum) to difference in the apparent pK_a of the phosphate moiety. Phosphate moieties typically have pK_a values around 7.0. In this case the inner-leaflet PA pK_a is shifted to a value larger than 12. Such a shift in pK_a may arise from packing the inner-leaflet PA headgroup in the concave surface. Close packing of the hydrocarbon tails will reduce the area available for the headgroup phosphate. In this smaller area fitting two negative charges is less electrostatically favorable than fitting one negative charge. The outer-leaflet PA headgroup is in a more relaxed geometry. This rationalization is consistent with what Hauser and coworkers have presented regarding the mechanism of spontaneous vesicle formation from PA dispersions subjected to a pH jump of 3–5 pH units [17,18]. In the case of vesicles produced by the pH-jump method, the pH gradient across the bilayer may be regarded as the driving force of the spontaneous formation of highly curved vesicles in which a larger electrostatic repulsion exists between

the doubly charged PA molecules on the outer monolayer than between molecules on the inner monolayer. In the case of sonicated PA dispersions discussed in this study, energy input in form of ultrasonic radiation supplies the driving force which establishes and maintains the specific stable geometry of the SUV in which a packing asymmetry is generated between the inner and outer leaflets.

This packing asymmetry translates into a difference in the ionization state of PA on both sides; a monoanionic form being energetically and electrostatically more favorable on the inside than a dianionic form. As we titrated SUVs of PA/PC mixtures prepared by sonication at pH 7.4 with NaOD and DCl, the observation that the outer-PA ^{31}P signal shifts towards and meets with the inner-PA signal at the acidic end of the titration curve (Fig. 7) indicates that the inner PA is primarily in a monoanionic form at pH 7.4. This ionization state was maintained by the inner PA even at pH 13.0 (Fig. 5), indicating a very high apparent pK_a in those molecules. Therefore, the process of generating the curved SUV surface is inseparable from the formation of a difference in the ionization state of PA on both sides of the bilayer whether the driving force is a pH gradient or ultrasonic energy. The larger the size of the vesicle the less the surface curvature, the smaller the asymmetry in molecular packing in the bilayer, the farther apart the molecules on the inner leaflet and thus the lower the pK_a, i.e., the easier it is for dianionic PA to form on the inside. This is also consistent with the observed dependence of the pK_a of the outer-leaflet PA on the amount of neutral PC present in the bilayer (Fig. 8). PC molecules act as separators that minimize the charge repulsion of PA. When mixed with PA, the PC molecules keep the charged PA headgroups farther apart, reducing the surface charge density on the membrane and thus yielding an apparently lower pK_a.

Inconsistent with our results are existing reports of single rather than double ^{31}P PA resonances in low-field studies of small unilamellar vesicles prepared by sonicating saturated-phosphatidate dispersions in H_2O at pH 7.3 [17,18]. The discrepancy is likely due to the different conditions used in each study. In the present work the bilayers were kept in a liquid-crystalline state in highly buffered solutions. In previous work, gel-state PA vesicles in non-buffered solutions were examined. It is possible that without a mediating buffer the proton exchange between solution and the phosphate moiety is sufficiently slow to lead to line broadening at a pH close to the pK_a of PA. Such ^{31}P-NMR line broadening has been observed in pH titration studies of micellar PA when the solution pH was close to the pK_a value of micellar PA (Garigapati, V.R., Bian, J. and Roberts, M.F., unpublished data).

The importance of PA-containing SUVs comes from the ability to differentiate in the NMR the internal and external membrane surfaces at physiological pH without the need for paramagnetic ions. In addition, they provide a probe of curvature – two distinct PA ^{31}P-NMR resonances – that is unaffected by the presence of calcium.

Acknowledgements

We thank Drs. David Atkinson and Donald Gantz for help with electron microscopic experiments and Dr. John Boylan of the Boston College NMR Facility for help with NMR experiments. This work was supported by NIH grants GM-44554 (to B.A.S.) and GM-26762 (to M.F.R.).

References

[1] Bangham, A.D., Standish, M.M. and Watkins, J.C. (1965) J. Mol. Biol. 13, 238–252.
[2] Reeves, J.P. and Dowben, R.M. (1969) J. Cell. Physiol. 73, 49–57.
[3] Papahadjopoulos, D., Vail, W.J., Pangborn, W.A. and Poste, G. (1976) Biochim. Biophys. Acta 448, 265–283.
[4] Papahadjopoulos, D. and Watkins, J.C. (1967) Biochim. Biophys. Acta 135, 639–652.
[5] Olson, F., Hunt C.A., Szoka, F.C., Vail, W.J. and Papahadjopoulos, D. (1979) Biochim. Biophys. Acta 557, 9–23.
[6] Paddy, M., Dahlquist, F., Davis, J. and Bloom, M. (1981) Biochemistry 20, 3152–3162.
[7] Frederik, P.M., Burger, K.N.J., Stuart, M.C.A. and Verkleij, A.J. (1991) Biochim. Biophys. Acta 1062, 133–141.
[8] Lenting, H.B.M., Nicolay, K. and Van den Bosch, H. (1988) Biochim. Biophys. Acta 958, 405–415.
[9] Tyrrell, D.A., Heath, T.D., Colley, C.M. and Ryman, B.E. (1976) Biochim. Biophys. Acta 457, 259–302.
[10] Finer, E.G., Flook, A.G. and Hauser, H. (1972) Biochim. Biophys. Acta 260, 49–59.
[11] Sheetz, M.P. and Chan S.I. (1972) Biochemistry 11, 4573–4581.
[12] De Kruijff, B., Cullis, P.R. and Radda, G.K. (1975) Biochim. Biophys. Acta 406, 6–20.
[13] Wilschut, J., Düzgünes, N., and Papahadjopoulos, D. (1981) Biochemistry 20, 3126–3133.
[14] Ames, B.N. and Dubin, D.T. (1960) J. Biol. Chem. 235, 760–775.
[15] MacDonald, R.C., MacDonald, R.I., Menco, B.Ph.M., Takeshita, K., Subbarao, N.K. and Hu, L. (1991) Biochim. Biophys. Acta 1061, 297–303.
[16] Kerker, M. (1969) The Scattering of Light, Academic Press, New York.
[17] Hauser, H., Mantsch, H.H. and Casal, H.L. (1990) Biochemistry 29, 2321–2329.
[18] Hauser H. (1989) Proc. Natl. Acad. Sci. USA 86, 5351–5355.